IL NUOVO CIMENTO **39 C** (2016) 416
DOI 10.1393/ncc/i2016-16416-5

COLLOQUIA: SWGM 2015

Irreversible aggregation of silica colloidal particles in binary solvent of 2,6-lutidine and water

ZHIYUAN WANG(1)(2), HONGYU GUO(2)(3), KATHERINE BORNER(2)(4) and YUN LIU(2)(3)(*)

(1) *Department of Engineering Physics, Tsinghua University - Beijing, China*
(2) *Center for Neutron Research, National Institute of Standards and Technology - Gaithersburg, MD 20899, USA*
(3) *Department of Chemical and Biomolecular Engineering, University of Delaware - Newark, DE, USA*
(4) *Department of Chemistry, The University of Texas at Dallas - Richardson, TX, USA*

received 6 July 2017

Summary. — Small silica colloidal particles suspended in a binary solvent, such as water and 2,6-lutidine, have attracted increasing attention in the past several decades as model systems to study critical adsorption, critical Casimir force, and colloidal glass transitions because the preferential solvent adsorption and the effective interaction between these colloidal particles can be tuned by controlling the temperature and solvent concentrations. In these early studies, the aggregation or clustering of particles driven by the solvent fluctuation is believed to be stable and thermally reversible. However, we demonstrate here conclusively that irreversible aggregates and gels can occur for silica nanoparticles in the binary solvent 2,6-lutidine and water when either the lutidine concentration or particle volume fraction is high enough. Hence, the interpretation of the experiment results needs to be taken into consideration when using such systems as model thermally reversible colloidal systems.

1. – Introduction

Since the first observation of the solvent fluctuation induced thermally reversible aggregation of silica particles dispersed in the lutidine/water mixture in 1985 [1], spherical silica colloidal particles suspended in different binary solvents have attracted a lot of attention as model systems to study critical adsorption, critical Casimir force, and glass transitions as the adsorption of solvent layers on the particle surfaces and the effective

(*) E-mail: yunliu@udel.edu, yun.liu@nist.gov

interactions between colloidal particles are controllable. Many experiments show that the thermally reversible aggregation happens when the binary liquid is approaching its phase separation temperatures [2-5]. Despite the plethora of investigations, the cause of the reversible aggregation is still a topic under debate. Theories such as critical adsorption [6, 7], wetting phenomena [7-10] and critical Casimir force [11, 12] are applied to explain these phenomena.

During all experimental reports, one of the basic assumptions taken as granted is that such aggregation is thermally reversible. However, thermally irreversible aggregation may also happen in some situations which make this assumption questionable. And thus the interpretation of some results becomes more complicated. It has been reported that polystyrene suspended in lutidine and water mixture will aggregate irreversibly if the sample temperature is 10 °C higher than phase separation temperature [12]. Another experiment also showed that when concentration of both silica colloidal particles and light mineral oil are high enough, irreversible aggregates appear in solutions [4]. The detailed reasons for the irreversible aggregation in these systems remain unclear.

While most papers did not mention the specific procedure through which they prepare samples, some papers mentioned that samples were prepared by diluting colloidal particles with adding binary solvent components separately [2, 13], and some other papers reported that they prepared samples by mixing binary components to mixture first and then adding colloidal particles [4, 5, 12]. When there are irreversible aggregates, the interpretation of some experiment results has to be much more careful. Therefore, it is important to understand the conditions favoring the formation of irreversible aggregates and avoid the possibility of having these types of aggregates.

In this paper, we systematically study silica colloidal particles in the mixture of water and 2,6-lutidine and conclusively show that significantly increasing the concentration of either lutidine or silica colloidal particles can induce irreversible aggregates. These irreversible aggregates are affected by the sample preparation methods. We propose the reasons for the formation of irreversible aggregates, from which a desired sample preparation method is suggested for silica colloidal particles in the mixture of lutidine and water.

2. – Theories and experiment methods

Dynamic light scattering (DLS) was used to measure the relaxation time of our samples, from which the hydrodynamic radius of particles can be obtained. DLS measures intensity autocorrelation function (IAF), which is defined as [14]

$$g_2(\tau, Q) = \frac{\langle I(t)\, I(t+\tau)\rangle}{\langle I(t)\rangle \langle I(t+\tau)\rangle}. \tag{1}$$

Here $g_2(\tau, Q)$ is IAF, $I(t)$ is the measured intensity of the DLS at time t, τ is the delay time, and Q is the scattering wave vector, which is defined as $Q = \frac{4\pi n}{\lambda}\sin(\frac{\theta}{2})$ (n is the solvent refractive index, λ is the laser wavelength, and θ is the detector angle). When the Seigert relationship is applicable, $g_2(\tau, q)$ can be linked to the intermediate scattering function (ISF) by the following equation:

$$g_2(\tau, Q) = 1 + \beta\,|g_1(\tau)|^2\,. \tag{2}$$

Here $g_1(\tau)$ is ISF, and β is the Seigert factor. At relatively dilute solutions, particles in solutions experience the diffusive motions, and the hydrodynamic radius can be then calculated through the well-known Stokes-Einstein relation. In this case, the ISF is a simple exponential function that can be expressed as

$$g_1(\tau) = \exp(-\Gamma\tau), \tag{3}$$

where

$$\Gamma = DQ^2, \tag{4}$$

and

$$D = \frac{kT}{6\pi\eta r}. \tag{5}$$

Here Γ is the decay rate of $g_1(\tau)$, D is the diffusion coefficient, k is the Boltzman constant, T is the absolute temperature, η is the solvent viscosity, and r is the hydrodynamic radius. If there is more than one population in a dilute particle suspension, $g_1(\tau)$ can be written as the summation of the contribution to the ISF from different populations as follows:

$$g_1(\tau) = \sum_i A_i \exp(-\Gamma_i\tau), \tag{6}$$

where

$$\sum_i A_i = 1. \tag{7}$$

The used silica particles (Ludox TM-50) and 2,6-lutidine were purchased from SIGMA-ALDRICH [15]. Milli-Q water (18.2 MΩ cm) was used in the preparation of all samples [15]. For samples of dilute silica particle (volume fraction $\phi = 1\%$) with the mixture of lutidine and water, two methods were used to prepare samples: Method 1 (M1) consists in simply mixing ludox with water first, and then adding lutidine directly to the solution. Method 2 (M2) consists in premixing lutidine and water, then diluting ludox with water, then mixing the diluted lutidine and silica particle solutions together as the last step. For lutidine concentration (c_l) from 15 wt% to 40 wt%, these 2 methods have not shown obvious differences, while for $c_l = 50$ wt%, there is a big difference. We will focus on this lutidine concentration for the diluted sample in the following data analysis.

The small angle neutron scattering (SANS) experiments were performed to obtain the shape and size of silica particles on NGB10m and NGB30m at the Center for neutron research in the National Institute of Standards and Technology. The SANS scattering intensity, $I(Q)$, can be written as

$$I(Q) = \phi\Delta\rho^2 V P(Q) S(Q) + I_b. \tag{8}$$

Here ϕ is the volume fraction of the particle, $\Delta\rho$ is the scattering length density contrast between the particle and solvent, V is the single particle volume, $P(Q)$ is the form factor, $S(Q)$ is the structure factor, and I_b is the intensity background from incoherent scattering.

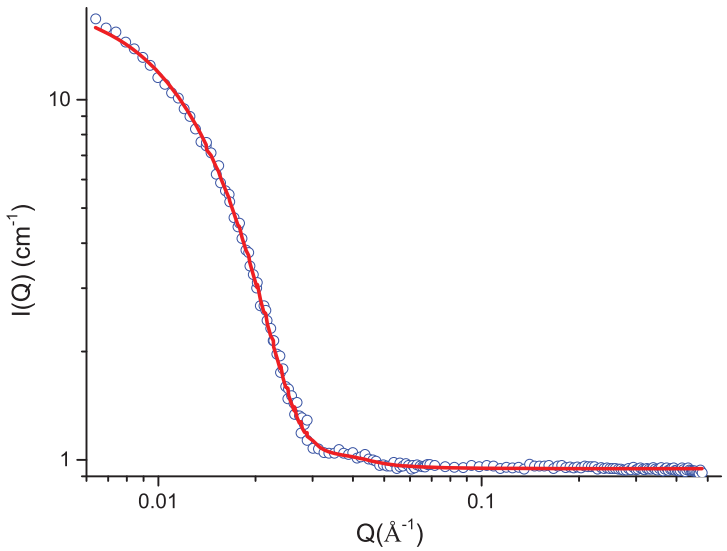

Fig. 1. – SANS scattering intensity of 0.1% volume fraction silica suspended in water and its fitted curve. The open circles are SANS data while the solid line is the fitted curve. The error bars are less than the size of symbols.

3. – Results and discussions

The purchased silica particles were first investigated using SANS by measuring 0.1% volume fraction of silica particles in water. The sample was prepared by simply diluting the silica particles from the purchased concentration. In order to fit the SANS pattern, silica particles are modeled as spherical particles with a Schultz distribution [16] for its particle size with mean radius r, and width σ_R. During the fitting, the scattering length density for the particle and solvent, and volume fraction for the particle are all fixed as the predetermined values. The scattering length density, ρ, of the silica particle has been measured to be $3.46 \times 10^{-6}\,\text{Å}^{-2}$ based on the value determined previously by our group [17]. As ϕ is small for the sample investigated with SANS, $S(Q) \approx 1$. Hence, there are only 3 fitting parameters, which are the particle size, the polydispersity width, and the background. The scattering intensity data (open circles) and its fitted curve (solid line) are shown in fig. 1. The obtained values are 13.8 nm, 2.28 nm for the mean radius r, and polydispersity width, σ_R, respectively. The background, I_b, is $0.95\,\text{cm}^{-1}$, which is mainly due to the incoherent scattering of protons from water. Therefore, the silica particle in solutions has relatively small polydispersity.

As the DLS is very sensitive to the particle aggregation, it is used to study the irreversible aggregation behaviors due to the sample preparation procedure difference. The lutidine concentration in solvent and the silica particle concentration in solution studied in the literature have a wide range. Since our silica particle surface preferentially adsorb water as determined previously by our group [17], the aggregation behaviors for silica particles appear on the lutidine rich side. Hence, we focus mainly on the lutidine concentrations higher than its critical concentration, 29 wt%.

We first examined the extreme situations where the lutidine concentration is relatively high. Here silica particles with 1% volume fraction were investigated first in the binary solvent with 50 wt% lutidine mass fraction. Right after the preparation, the samples prepared with both M1 and M2 methods were initially transparent. However, for the

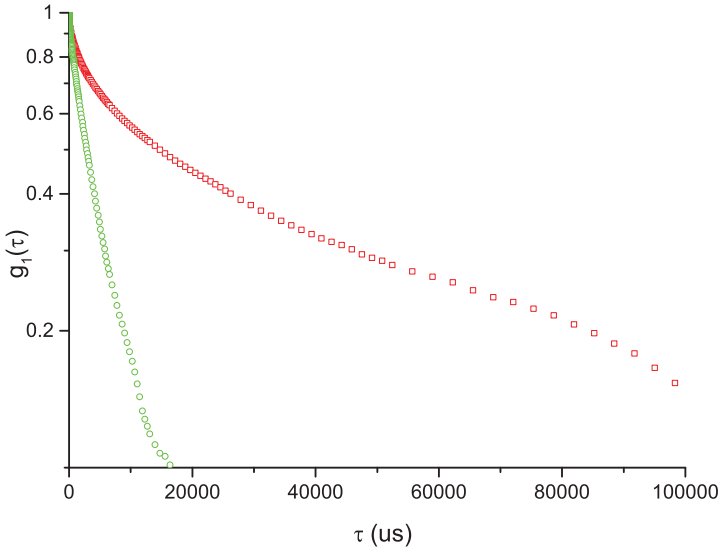

Fig. 2. – The intermediate scattering functions (ISFs) for samples using different preparation methods after preparation for 2 hours. The x-axis is in linear scale while the y-axis is in log scale. The red squares are for the sample treated with M1-0, while the green squares are for the sample treated with M2-0.

sample prepared with the M1 method, after about 48 hours, there were clear white colored precipitates at the bottom of the sample vial while the samples prepared with the M2 method remained a clear solution. It is therefore clear that the M1 method introduces some irreversible aggregates. It is noted that the final constituent concentrations for samples prepared with both M1 and M2 are identical. The only difference was the preparation procedures. Therefore, the irreversible aggregates introduced by M1 is solely affected by the preparation procedure.

We have tried to investigate if the irreversible aggregates can be dissolved by applying some physical methods. Hence we used both the vortex-shaker and sonicator. Different measurements are labeled typically as Mx-y, where Mx means the sample is prepared first with Mx method and y indicates the experiment method number this sample was treated before a DLS measurement. For Mx-0, the samples were measured just right after preparing with the Mx method for 2 hours without any further treatment. For Mx-1, after white precipitates occurred in the solution, the sample was shaken with the vortex-shaker for 16 hours at relative low speed; for Mx-2, the sample was first treated in Mx-1, and was then taken out and put into the bath of a sonicator for 1 hour; for Mx-3, the sample treated after the Mx-2 step was further to be put in sonication for 1 extra hour.

For samples prepared with the M1 method, after the treatment of M1-1, the samples become turbid without visible large precipitates for a very long time, which means the precipitates may be broken into smaller aggregates and partially dissolve in the solvent. After the treatment of M1-2, the samples become less turbid. The treatment of M1-3 can make the final solutions transparent. Hence, the formed irreversible aggregates may not be bound very strongly. By these physical mixing methods, we can still break them.

DLS is used to probe the aggregation behaviors of our samples. The $g_1(\tau)$ from DLS measurement of M1-0 and M2-0 are shown in fig. 2. Clearly, right after the preparation,

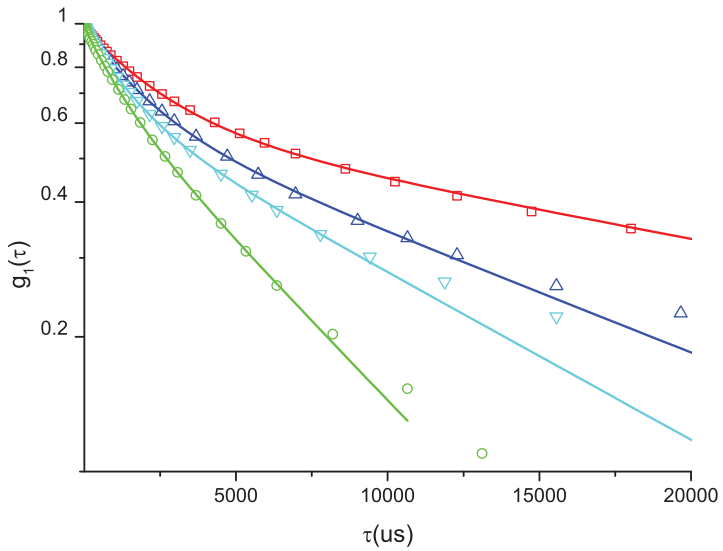

Fig. 3. – The intermediate scattering functions (ISFs) for each sample after different sample treatments together with their fitted curves. The x-axis is in linear scale while the y-axis is in log scale. Red squares are for the sample treated with the M1-1. Blue up triangles are for the sample treated with the M1-2. Teal down triangles are for the sample treated with the M1-3. Green circles are for the sample treated with the M2-1. The error bars representing one standard deviation are less than the size of symbols.

the sample prepared with the M1 method has large aggregates as indicated by the slow decaying curve (red squares) even though the sample was transparent at the beginning.

Figure 3 shows the $g_1(\tau)$ from DLS measurement of M1-1, M1-2, M1-3 and M2-1. As M2-2 and M2-3 show no difference with M2-1 from DLS result, the $g_1(\tau)$ of M2-2 and M2-3 are not put in fig. 3. From figs. 2 and 3 it is clear that for the samples with the same concentration with different preparing methods, the samples dynamic are different. Comparing M1 and M2 data, samples prepared with the M1 method has much slower decay, indicating that the average particle size is larger in the sample prepared with the M1 method. Therefore, there are larger aggregations in these samples prepared with the M1 method. Based on this decaying curve only, it is still not clear if there are no irreversible aggregates in the M2-1 sample. However, it definitely has less aggregates compared with that prepared with the M1 method. On the other hand, even after the treatment of the samples using M1-3, while the solution can change from turbid to transparent, the decay rate is still slower than that of M2-1. This indicates that even though the aggressive shaking and sonication can break large irreversible aggregates, there are still large amounts of small irreversible aggregates in solutions that cannot be broken with our methods.

In order to quantitatively understand $g_1(\tau)$, we have attempted to analyze the decay curves using three exponential decays to fit the data. These three exponentials are used to represent the decay due to pure solvent (Γ_1), small silica particle aggregates including monomers (Γ_2), and large silica particle aggregates (Γ_3). Γ_2 is the decay caused by the average results of monomers and small aggregates as it is difficult to separate the effect of monomers from those small aggregates. Γ_3 is used to investigate the large aggregates

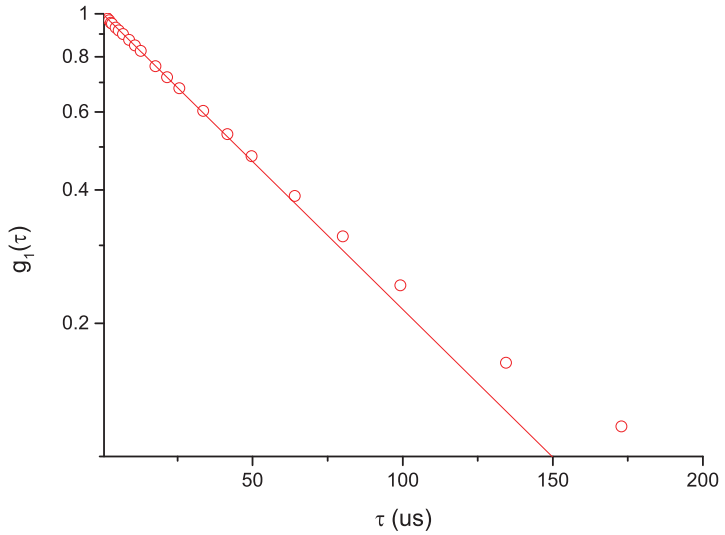

Fig. 4. – The intermediate scattering function $g_1(\tau)$ of lutidine and water mixture of $c_l = 50\,\mathrm{wt}\%$ and its fitted curve. The x-axis is in linear scale while the y-axis is in log scale. Open circles are experiment data.

formed in solutions. To estimate the decay rate of the pure solvent (Γ_1), $g_1(\tau)$ of lutidine and water mixture of $c_l = 50\,\mathrm{wt}\%$ without silica nanoparticles is measured. The result $g_1(\tau)$ is shown in fig. 4. The decay rate obtained from fig. 4 is much slower compared to the single molecule motions in either pure lutidine or water. Hence, this indicates that water and lutidine are not perfectly mixed. There are certain structures formed by water in lutidine.

Based on the fitting of the pure solvent, we thus fixed the value (the decay rate) for Γ_1 as the value obtained from fig. 4 when analyzing the $g_1(\tau)$ for the samples with silica particles. Corresponding fitted curves are shown with data in fig. 3. Table I shows the fitted decay rate for the samples of $\phi = 1\%$ and $c_l = 50\,\mathrm{wt}\%$ using the M1 and M2 methods mentioned previously. The quantitative values we obtained are consistent with our previous observations discussed above. Γ_3 is the smallest value among Γ_1, Γ_2 and Γ_3 as it is due to the formation of large silica aggregates. With longer shaking and sonicating time after samples are treated by M1-2 and M1-3, Γ_2 and Γ_3 increase, which is consistent with the discussion above that some of the aggregates are broken by vigorously shaking and sonicating the samples for long time. However, the decay rate is still much smaller than that measured for the M2-1 sample. Therefore, there are still irreversible aggregates even after using shaking methods. Hence, for samples of high lutidine concentrations prepared by the M1 method, some irreversible aggregation is inevitable.

We have attempted to further estimate the hydrodynamic radius based on the decay rate. However, it is important to point out that the application of the Stokes-Einstein relation requires that all solvent structures should be significantly smaller than the size of diffusive particles in the solution. Since the solvent does form structures in the solution, it is still questionable if we can apply the Stokes-Einstein relation to estimate the hydrodynamic radius. This has also been pointed out by an earlier paper too [18]. But we feel

TABLE I. – *The fitted decay rate of samples of $\phi = 1\%$ and $c_l = 50\,wt\%$ with two methods and different measurements.*

Sample label	$\Gamma_1(s^{-1})$ (fixed)	Γ_2 (s^{-1})	Γ_3 (s^{-1})
M1-1	1.54×10^4	$(2.97 \pm 0.09) \times 10^2$	$(1.94 \pm 0.07) \times 10^1$
M1-2	1.54×10^4	$(3.64 \pm 0.12) \times 10^2$	$(3.79 \pm 0.16) \times 10^1$
M1-3	1.54×10^4	$(4.45 \pm 0.13) \times 10^2$	$(5.15 \pm 0.21) \times 10^1$
M2-1	1.54×10^4	$(5.92 \pm 0.46) \times 10^2$	$(16.82 \pm 0.91) \times 10^1$

that the hydrodynamic radius obtained in this way is still informative to understand our systems.

The refractive index and viscosity of the pure mixture of lutidine and water have been measured and reported for different temperatures [18, 19]. In order to obtain the values at our DLS laser wavelength, 663 nm, and temperatures, 25 °C, linear interpolation was used. The obtained results are listed in table II for our cases. Using the information in table II, we have estimated the average hydrodynamic radius of the particle aggregates in our samples. Even the solution was transparent after the treatment of M1-3, the estimated hydrodynamic radius using Γ_3 is about 427 nm. However, the total number density for these large aggregates is very small. The dominating species are small aggregates together with monomers, whose average hydrodynamic radius can be determined from Γ_2. The estimated size is about 49 nm. This is significantly larger than 13.8 nm determined using SANS. As a comparison, the hydrodynamic radius obtained from Γ_2 with the M2-1 method is about 37 nm. And we also attempted to estimate the hydrodynamic radius of the pure water structure in lutidine which is on the order of 2 nm. This hydrodynamic radius of the water structure in solution may not be accurate. But it shows that the time scale of the dynamics of the solvent molecules is comparable to that of the motions of small silica particle aggregates given the true size of the particles obtained from SANS. Therefore, the particle radius extracted from Γ_2 using the Stoke-Einstein relation may only be discussed in a qualitative way. The real particle size is more accurately determined by SANS.

Having shown that the preparation method matters a lot for the irreversible aggregates formation for lutidine concentration $c_l = 50\,\mathrm{wt}\%$, we have also tried to investigate the

TABLE II. – *The viscosity and refractive index of water and lutidine mixture with different lutidine concentration at* 25 °C *and* 663 nm *light wavelength. The numbers are coming from linear interpolation* [18, 19].

Lutidine mass fraction c_l/wt%	Viscosity η/cP	Refractive index n
15	1.57	1.359
29	2.43	1.383
40	3.46	1.406
50	3.92	1.425

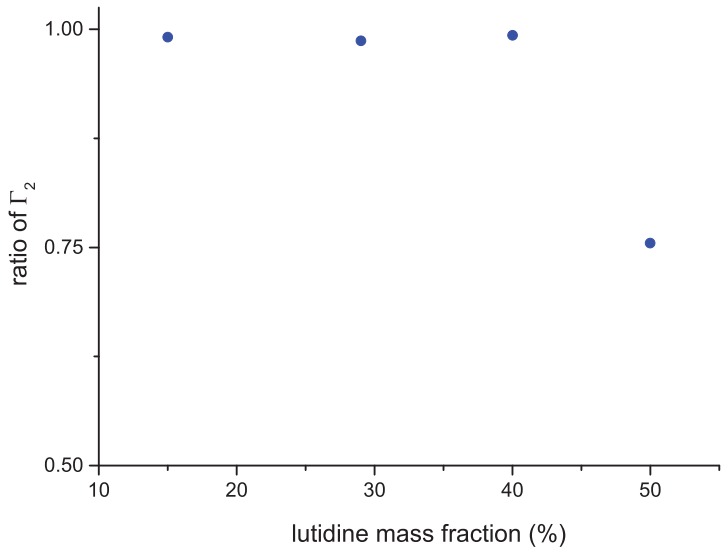

Fig. 5. – Ratio of fitted Γ_2 of $\phi = 1\%$ silica particles suspended in a solvent of water and lutidine with different c_l between the M1 and M2 method. The blue dots are the ratio of fitted Γ_2 between M1 and M2 method.

effect of the lutidine concentration using the methods in the case with $c_l = 50\,\mathrm{wt}\%$. The lutidine concentration c_l from 15 wt% to 40 wt% were investigated by preparing the samples using the M1 and M2 method with DLS. Similarly to the case of samples of $c_l = 50\,\mathrm{wt}\%$, we have measured the decay rate of lutidine/water mixture which can be used in the fitting. We used three fitting exponential functions. The amplitudes of Γ_3 were found very close to 0, giving us an unreasonable Γ_3 in the fitting. It also means that big aggregation only occurs when c_l is higher than 40 wt%. Since we would like to focus on the dominating species (monomer and small aggregates), we will discuss the results mainly obtained from Γ_2. Figure 5 shows the Γ_2 ratio between M1 and M2 methods for samples of different c_l. We can see that the ratio is almost 1 when $c_l \leq 40\,\mathrm{wt}\%$. Almost no differences between these two methods are observed. Hence, even though the M1 method introduces irreversible aggregates in solutions at $c_l = 50\,\mathrm{wt}\%$, it introduces less irreversible aggregates in solutions when the c_l decreases. It is clear that the irreversible aggregate is very sensitive to the lutidine concentration.

The irreversible aggregation of silica particles is a process-dependent phenomenon. We can use the "DLVO-like" potential to explain this effect. The DLVO principle was first developed by Derjaguin [20], then extended with Landau [21], polished by Verwey and Overbeek [22]. The theory was first proposed for two identical interfaces, then extended to two different interfaces. The reason we call it "DLVO-like" not DLVO is that in our system the Van der Waals attraction may not dominate the attraction. The solvent-mediated attraction can be significantly contributing to the attraction, which is different from the DLVO assumption. However, the distance dependence of the total potential is still similar. Before mixing with lutidine, the interaction between silica particles has a huge repulsive energy barrier due to the electrostatic repulsion that stabilizes the suspension. This is the reason why the volume fraction of silica nanoparticles from Ludox TM-50 can be as high as 30% without any aggregation. Meanwhile, there is a

huge attractive potential well in very short particle-particle distance which is possibly due to the chemical bond of silica particles, and the chemical bond is thermal irreversible. When we change the solvent condition, the solvent-mediated attraction, similar to the critical Casmir force, will affect particle-particle potential. There is a secondary minimum potential where reversible aggregation forms. The reversible aggregation increases the local concentration in these aggregates so that the chance for the irreversible aggregates increases dramatically.

For the M1 and M2 method, all samples were prepared at 25 °C, far from the critical temperature. However, for the M1 method, the lutidine is added to the silica particle solutions as the last step. It is known that when mixing the lutidine with water, the temperature of the binary solvent increases due to the released heat by the mixing. Thus, even if the lab temperature is kept at 25 °C, the sample can be heated to a higher temperature temporarily. When the temperature increases, it has been shown that the binary solvent introduced attraction between silica particles can become stronger [23] and introduce more reversible aggregation. On the other hand, for the M2 method, the lutidine is first mixed with water without the silica particles. When the silica particle solution is added to the binary solvent of the lutidine and water, the potential temperature change of the solution is much smaller. Hence, the solvent introduced attraction is so small that the particles will not be so close to each other. Therefore, the irreversible aggregation we observed due to the solvent-mediate attraction may reduce the energy barrier which may lead more particles drop to the primary attraction well close to the particle surface. The amount of the irreversible aggregation is different depending on the way we prepare samples. Comparing with Method 1 and Method 2, we know that if we want the sample to have the lowest irreversible aggregation, it is important to limit high local concentration of lutidine when preparing the sample.

For a $\phi = 1\%$ silica sample in the binary solvent, higher lutidine concentration in the solvent favors the formation of irreversible aggregates. At low silica particle concentrations, the clear precipitated aggregates are only observed for c_l higher than 40 wt%. It may be argued that the irreversible aggregation only happens to the off-critical lutidine concentration where there are large amounts of lutidine. From our discussion by "DLVO-like" potential, the formation of irreversible aggregation only depends on the energy barrier and the possibility that the particles pass through the repulsive barrier to interact with the strong attractive potential well. To test this speculation, samples of critical and near critical concentration of lutidine are prepared with a high volume fraction of silica particles. By increasing the number density of the silica particles, we increase the chance for the particles to get over the repulsive barriers. Figure 6 shows that after leaving the samples of $\phi = 15\%$ silica suspended in the lutidine and water mixture at 20 °C for one day without any treatment, irreversible gelation can be seen clearly, which means that at a high volume fraction of silica, the interaction between silica particles is also different in the lutidine/water mixture compared with silica suspended in pure water. This further supports out previous speculations that the irreversible aggregates observed here are intrinsic to the silica particles we studied, and the amount of irreversible aggregates depends on the sample preparation procedures.

Even though we show here that for certain solvent conditions, the irreversible aggregates are inevitable for the Ludox silica particles in the binary solvent of lutidine and water, which are commonly used as a model system to study reversible glass transition and aggregations, we also noticed that the formation of irreversible aggregates is a relatively slow process. For the large particle concentration case ($\phi = 15\%$), it takes at least one day for the samples to become gel. Hence, for the samples prepared at low

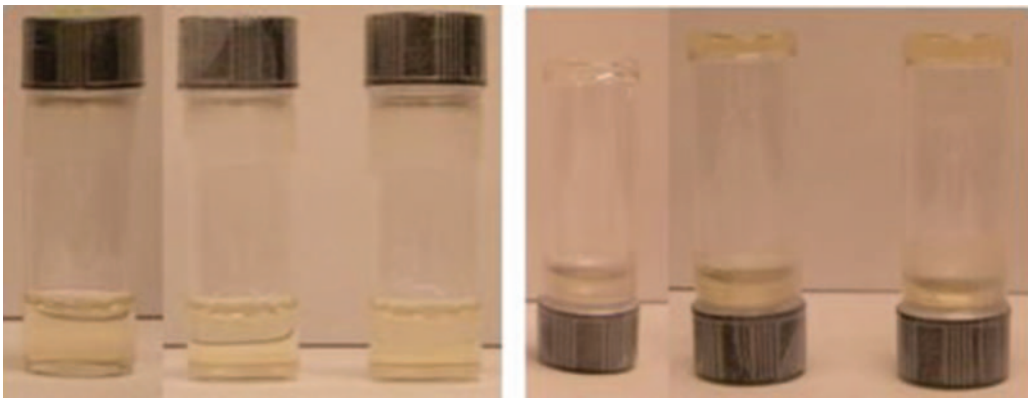

Fig. 6. – The gelation of $\phi = 15\%$ in critical- and near-critical-concentration lutidine. Left: the solvent mixture is shown; right: we put the bottle upside down and then we can see gelled solid phase at the bottom of the bottles clearly. Lutidine concentration c_l from left to right is 29 wt%, 31 wt% and 33 wt%, respectively.

lutidine concentration, the samples can be considered as still dominated by reversible aggregates compared to irreversible aggregation if the experiments are done in short time. Certainly, a high lutidine concentration favors the formation of irreversible aggregates; for the case of the low particle concentration ($\phi = 1\%$) for $c_l = 50$ wt%, the sample prepared with the M1 method did not immediately show white precipitates. But the DLS data indicate that there are already large aggregates even though there are no precipitates. The white precipitates are observed clearly after a couple of days.

4. – Conclusion

The formation of irreversible aggregates in silica nanoparticles suspended in the binary solvent of 2,6-lutidine and water is systematically studied at room temperature. It is found that high lutidine concentration favors the formation of irreversible aggregates, which depends on the sample preparation methods. A "DLVO-like" potential can be used to explain why thermally irreversible aggregation occurs. This speculation is also consistent with the observation of gelled solid phase when the samples have a high volume fraction of silica particles. Based on our experiments, the local temperature increase due to the mixing of the lutidine and water plays an important role for the irreversible aggregation for samples with small silica particle concentrations. Therefore, a good sample preparation method (M2 method) to avoid the irreversible aggregation is proposed to limit irreversible aggregation at high concentration of lutidine during the preparation of a sample. However, when particle concentration is high, the irreversible aggregates can even happen at relatively low lutidine concentrations. We also observe that when samples are prepared with the M1 method, the formation of irreversible aggregates at small lutidine concentration seems to be a slow process. Hence, if an experiment can be performed in a short time after a sample is prepared, the sample can be still considered to be thermally reversible and dominated by thermal reversible aggregates when the sample temperature is close to the demixing temperatures of the solvent.

* * *

This manuscript is prepared with the partial support of cooperative agreements 70NANB12H239 and 70NANB10H256 from NIST, U.S. Department of Commerce. This work utilized facilities supported in part by the National Science Foundation under Agreement No. DMR-0944772.

REFERENCES

[1] Beysens D. and Esteve D., *Phys. Rev. Lett.*, **54** (1985) 2013.
[2] Narayanan T., Kumar A., Gopal E. S. R. *et al.*, *Phys. Rev. E*, **48** (1993) 1989.
[3] Kurnaz M. L. and Maher J. V., *Phys. Rev. E*, **51** (1995) 5916.
[4] Heidlebaugh S. J., Domenech T., Iasella S. V. *et al.*, *Langmuir*, **30** (2014) 63.
[5] Hijnen N. and Clegg P. S., *Langmuir*, **30** (2014) 5763.
[6] Law B. M., Petit J. M. and Beysens D., *Phys. Rev. E*, **57** (1998) 5782.
[7] Law B. M., *Prog. Surf. Sci.*, **66** (2001) 159.
[8] Sluckin T. J., *Phys. Rev. A*, **41** (1990) 960.
[9] Bauer C., Bieker T. and Dietrich S., *Phys. Rev. E*, **62** (2000) 5324.
[10] Schlesener F., Hanke A. and Dietrich S., *J. Stat. Phys.*, **110** (2003) 981.
[11] Bonn D., Otwinowski J., Sacanna S. *et al.*, *Phys. Rev. Lett.*, **103** (2009) 156101.
[12] Gallagher P. D. and Maher J. V., *Phys. Rev. A*, **46** (1992) 2012.
[13] Van Duijneveldt J. S. and Beysens D., *J. Chem. Phys.*, **94** (1991) 5222.
[14] Berne B. J. and Pecora R., *Dynamic Light Scattering: With Applications to Chemistry, Biology, and Physics* (Dover Publications, New York) 2000, pp. 10–24.
[15] The statements, findings, conclusions and recommendations are those of the author(s) and do not necessarily reflect the view of NIST or the U.S. Department of Commerce.
[16] Aragon S. R. and Pecora R., *J. Chem. Phys.*, **64** (1976) 2395.
[17] Bertrand C. E., Godfrin P. D. and Liu Y., *J. Chem. Phys.*, **143** (2015) 084704.
[18] Stein A., Davidson S. J., Allegra J. C. *et al.*, *J. Chem. Phys.*, **56** (1972) 6164.
[19] Jayalakshmi Y., Van Duijneveldt J. S. and Beysens D., *J. Chem. Phys.*, **100** (1994) 604.
[20] Derjaguin B., *Prog. Surf. Sci.*, **43** (1993) 1.
[21] Derjaguin B. and Landau L., *Prog. Surf. Sci.*, **43** (1993) 30.
[22] Verwey E. J. W. and Overbeek J. T. G., *Theory of Lyophobic Colloids* (Elsevier Press, 1948).
[23] Hertlein C., Helden L., Gambassi A. *et al.*, *Nature*, **451** (2008) 172.